

See discussions, stats, and author profiles for this publication at:
<https://www.researchgate.net/publication/223744621>

Nondestructive waste-drum assay for transuranic content by gamma-ray active and passive computed tomography

Article in Nuclear Instruments and Methods in Physics Research Section A Accelerators Spectrometers Detectors and Associated Equipment · December 2002

DOI: 10.1016/S0168-9002(02)01315-3

CITATIONS

21

READS

92

5 authors, including:



[H.E. Martz](#)

Lawrence Livermore National Laboratory

141 PUBLICATIONS **514** CITATIONS

SEE PROFILE



ELSEVIER

Nuclear Instruments and Methods in Physics Research A 495 (2002) 69–83

**NUCLEAR
INSTRUMENTS
& METHODS
IN PHYSICS
RESEARCH**
Section A

www.elsevier.com/locate/nima

Nondestructive waste-drum assay for transuranic content by gamma-ray active and passive computed tomography

D.C. Camp^{a,1}, H.E. Martz^{b,*}, G.P. Roberson^b, D.J. Decman^b, R.T. Bernardi^c^aLawrence Livermore National Laboratory, Livermore, CA 94550, USA^bLawrence Livermore National Laboratory (LLNL), 7000 East Ave., Livermore, CA 94550, USA^cBio-Imaging Research, Inc., Lincolnshire, IL 60069, USA

Received 16 July 2001; received in revised form 29 April 2002; accepted 1 July 2002

Abstract

A gamma-ray-based, active (A) and passive (P) computed tomography (CT) technology has been developed that locates, identifies and quantifies gamma-ray emitting isotopes, transuranic (TRU) and others, in nuclear waste drums. ACT uses a collimated external source and a HPGe detector to measure selected mono-energetic gamma-rays that are attenuated by waste-drum contents; a separate PCT measurement uses the HPGe detector to record the spectra of gamma-rays emitted from within a drum. The ACT attenuation images and the PCT emission spectra are coupled to quantitatively assay drum contents for ~0.1–200 g of TRU isotopes. Calibration requires a single measurement of a known radioactive standard; construction of waste-drum surrogates is not required. Fixed and mobile systems demonstrated compliance with a DOE quality assurance program via several independent blind tests.

© 2002 Elsevier Science B.V. All rights reserved.

PACS: 28.41.K; 87.59.F; 87.58.C; 07.85

Keywords: Nondestructive assay; Transuranic isotopes; Gamma-ray spectroscopy; Active (transmission) and passive (emission) computed tomography

1. Introduction

Early nondestructive assay (NDA) approaches [1,2] for assaying transuranic (TRU) isotopes in waste drums adapted existing safeguards techniques, which measure ideal samples containing tens- to kilogram quantities of pure uranium (U) or plutonium (Pu) oxides, solutions or metal. These technologies and their assumptions are not

adequate for most heterogeneous wastes; and may give reasonable answers only if extensive calibrations are done using carefully constructed surrogate waste matrices. This is costly because it is not possible to construct all combinations of wastes.

Waste items in the US Department of Energy's (DOE) inventory have different matrix densities and compositions, different radionuclide and isotopic compositions; and different physical, chemical and distributional forms of radioactivity [3]. Some of these variables impact assay response and must be accounted for if valid measurements are desired. Most 208-l drums will be assayed

*Corresponding author. Tel.: +1-925-423-4269.

E-mail address: martz2@llnl.gov (H.E. Martz).

¹Consultant, LLNL, Livermore, CA, USA

noninvasively, because the analysis cost per opened drum is prohibitively expensive. Categories of radioactive wastes include contact-handled² TRU,³ low level (LLW),⁴ or mixed.⁵

At LLNL we developed a cost-effective technology that can assay waste drums independent of their content. It measures milligram amounts or more of TRU and other isotopes in defense, commercial or medical wastes. Assay times are adjustable to reflect activity content and/or waste density. Once calibrated our active (A) and passive (P) computed tomography (CT) technology corrects the measured radiations from internal sources for the attenuation of the waste matrix; and the technology identifies and quantifies all radioisotopes detected. The technology transfer to industry was done in cooperation with Bio-Imaging Research, Inc. (BIR) [4–6]. More recently, we developed a six-source and six-HPGe-detector system [7–9] to shorten drum scan times (≥ 30 min) compared to those discussed here; results for the six-detector system will be presented in a future paper.

Other NDA developmental efforts in the USA include neutron techniques [10–12], gamma-ray techniques [13–15], or a combination [16,17]. Some efforts outside the USA are given in Refs. [18–23]. Several of these [14,15,19–23] use a CT approach. Additional references on other NDA techniques used for waste drum analyses are given in Ref. [24]. All neutron-based NDA systems require waste matrix content and/or pre-calibration versus matrix content before their results can be interpreted. They also require relative isotopic ratios of any fissile–fertile elements, typically, plutonium, before their results can be interpreted. The waste matrix content and isotopics are usually determined from X-ray-based NDE and gamma-ray-based NDA systems, respectively.

²Contact Handled (CH) wastes are those having ≤ 200 mR/h at contact with the drum's surface.

³Transuranic wastes (TRU) are those with $Z \geq 92$, half-lives > 20 yr, activities ≥ 100 nCi/g of net waste weight; and less than 200 g of plutonium per 208-l drum.

⁴Low-level wastes are those defined as containing less than 100 nCi/g of net waste weight.

⁵Mixed wastes are those defined as containing both radioactivity and hazardous materials.

Of these techniques the one most similar to ours is tomographic gamma scanning (TGS) developed by Estep et al. [13]. Our approach uses imaging to obtain an absolute assay of radioactive isotopes independent of drum matrix content. Our technology uses a detector collimator aperture that is smaller than the detector's area and has a less complex response function; we obtain higher spatial resolution and scan in a discrete step-wise fashion for a variable assay time vs. their continuous scanning for a fixed time. We acquire the entire gamma-ray spectrum at every data acquisition position vs. their pre-selected energy regions, and the image reconstruction and assay algorithms we use are very different. TGS sometimes requires calibration using specially constructed waste drum surrogates, whereas our technology measures any matrix with only a single radioactive source calibration.

2. Technology theory

Conventional active or transmission CT scanners measure the effects of an object on an incident beam or “ray” that travels in a straight path [25–27]. In gamma-ray CT, $I_0[S(E), L]$ is the measured photon intensity of the incident beam and $I[S(E), L]$ is that of the transmitted beam attenuated by an object along each ray path, L , for a photon energy spectrum $S(E)$.

The quantity reconstructed in CT is the value of some function, $f[S(E), \mathbf{x}]$, for some volume element, or voxel, at location $\mathbf{x} = (x, y, z)$ within the object. The reconstruction algorithms require line integrals, also called ray sums, for many ray paths L , defined as

$$g[S(E), L] = \int_L f[S(E), \mathbf{x}] du \quad (1)$$

where du is the incremental distance along L . For gamma-ray CT, these ray paths are determined from the intensity measurements using the Beer's law relationship

$$g[S(E), L] = \ln \left[\frac{I_0[S(E), L]}{I[S(E), L]} \right]. \quad (2)$$

Ray sums over many paths are needed to reconstruct $f[S(E), \mathbf{x}]$.

2.1. Active computed tomography (ACT)

Conventional industrial CT scans use an X-ray source with a wide energy spectrum and a current-integrating detector that sum the energy deposited by photons over all energies. Our A&PCT nuclear-spectroscopy-based scanner discriminates between photons of different energies. The resultant image is given by

$$f(E, \mathbf{x}) = \mu[\rho(\mathbf{x}), Z(\mathbf{x}), E] \quad (\text{monoenergetic}). \quad (3)$$

The results are a discrete quantitative measurement of the linear attenuation coefficient, where ρ is volume density and Z is atomic number, at one energy E , and there is no integration over the energy spectrum, $S(E)$.

The ray path, L , is simplified if we consider a single 2D x - y plane fixed along the longitudinal axis, z , of a waste drum. We treat a single discrete gamma-ray beam in that plane as a linear ray path defined by s , the distance between the ray path and the $(x$ - $y)$ origin, and θ , the angle of the s axis from the x axis. The transmitted beam intensity $I(E, s, \theta)$ for this ray path at a fixed energy, E , is

$$\begin{aligned} I(E, s, \theta) &= I_0(E, s, \theta) \\ &\times \exp - \left[\iint \mu(E, x, y) \delta(x \cos \theta + y \sin \theta - s) dx dy \right] \end{aligned} \quad (4)$$

where $\mu(E, x, y)$ is the spatial distribution of the linear attenuation coefficients at energy, E ; I_0 is the intensity of the incident beam; and δ is the Dirac delta function. The ray path equation is $x \cos \theta + y \sin \theta - s = 0$. The argument of the exponential is a ray sum, $g(E, s, \theta)$, and is equal to

$$\begin{aligned} g(E, s, \theta) &= \ln \left[\frac{I_0(E, s, \theta)}{I(E, s, \theta)} \right] \\ &= \iint \mu(E, x, y) \delta(x \cos \theta + y \sin \theta - s) dx dy. \end{aligned} \quad (5)$$

In effect, the CT ray sum is analogous to a gamma-ray transmission gauge experiment.

The set of ray sums at all values of s at a given elevation (slice) for a fixed E and θ is called a “projection”, and a complete set of parallel-beam projections at all θ (from 0° to 180° or 360°) for a fixed E is called a “sinogram”. From measurements of I and I_0 , a complete ACT sinogram can be determined; and various methods have been devised to reconstruct μ , the linear attenuation coefficient, with filtered back projection (FBP) being the most common [25]. Therefore, μ is the parameter determined by image reconstruction of the ACT measurements at a *selected energy value* and voxel. For a waste drum, the attenuation due to drum contents is accurately measured in all three dimensions by acquiring and reconstructing ACT data at different z planes (or elevations) of the drum.

2.2. Passive computed tomography (PCT)

Passive CT measures the identity and quantity (uncorrected for attenuation) of the gamma-ray emitting radionuclides within a waste drum. The ray sum for passive or single-photon-emitted CT (SPECT) imaging, $g_\gamma(E, s, \theta)$, is defined by Budinger et al. [25] as

$$\begin{aligned} g_\gamma(E, s, \theta) &= I_e(E, s, \theta) \\ &= \iint \mathbf{p}(E, x, y) a(E, x, y, s, \theta) \\ &\quad \times \delta(x \cos \theta + y \sin \theta - s) dx dy \end{aligned} \quad (6)$$

where I_e are the passive or emission counts measured at each ray sum position and

$$\begin{aligned} a(E, x, y, s, \theta) &= \exp - \left[\int_x^{\text{detector}} \int_y^{\text{detector}} \mu(E, x', y') \right. \\ &\quad \left. \times \delta(x' \cos \theta + y' \sin \theta - s) dx' dy' \right] \end{aligned} \quad (7)$$

is the half-line attenuation integral from (x, y) position to the detector position defined by (s, θ) ; and $\mathbf{p}(E, x, y)$ are photons of energy E emitted per unit volume per unit time in a waste drum.

A single-photon-emitted ray sum is the integrated radioisotope activity, modified by one or a multiple of exponential attenuations, along the path from the source position within the drum to the detector. The influence of the term

$a(E, x, y, s, \theta)$ depends on the magnitude and distribution of the attenuations in a waste drum, which for most energies emitted are typically large and nonhomogeneous. To obtain accurate results from PCT measurements, the energy-dependent attenuations can be determined from ACT measurements. The commonly used assumption of an average attenuation is inadequate for accurate assays of inhomogeneous waste matrices.

2.3. Coupling active and passive computed tomography

Coupling ACT and PCT data allows accurate quantitative attenuation corrections to be applied to the emitted photons, \mathbf{p} , from a radioisotope at each voxel location. The activity for a particular gamma-ray, j , is determined from

$$C_j(E) = \sum_i p_i(E) \quad (8)$$

where $C_j(E)$ is the total photons per unit time obtained from the sum of all the voxels at energy E for the reconstruction of the passive CT data corrected by the ACT attenuation map. Once total photons are obtained, the activity, A^j , is obtained from

$$A^j(\text{mCi}) = \frac{C_j(E)}{t\varepsilon(E)\beta_j k} \quad (9)$$

where t is the ray sum integration time, $\varepsilon(E)$ is the high-purity germanium (HPGe) detector efficiency⁶ at energy E of the emitted gamma-ray measured, β_j is its branching ratio, and k is 3.7×10^7 disintegrations per second per milliCurie. The measured activity is converted to its gram value, m , using

$$m_j(g) = \frac{A^j}{A_{\text{sp}}^j} \quad (10)$$

where m_j is the mass in grams of radioisotope j , that has specific activity A_{sp}^j .

⁶ Does not include the solid angle. The solid angle is included in the image reconstruction and assay algorithm discussed in Section 3.

3. Image reconstruction codes

ACT data is acquired and reconstructed using a well-known 2D filtered backprojection method [25]. The resultant 2D ACT slice data at a particular energy is merged into a 3D array before being submitted with PCT data to the PCT image reconstruction and assay algorithm. Assay of a drum is divided into a set of voxels. The number of counts for all detectable isotopes is determined for each voxel (Eq. (6)). The counts from all voxels (Eq. (8)) determine the assay of the drum.

PCT image reconstruction and assay start by defining an unknown vector, \mathbf{p} , which is the desired solution and its element represent the number of counts from each voxel. The emitted radiation is measured at a series of detector positions, which constitute the ray sums in a passive CT scan. The vector, \mathbf{g}_γ (Eq. (6)), is the sinogram data measured in a PCT scan, and each vector element is measured radiation at a given detector position. The relation between the vectors \mathbf{p} and \mathbf{g}_γ is defined as

$$\mathbf{g}_\gamma = \mathbf{A}\mathbf{p}. \quad (11)$$

The system matrix, \mathbf{A} , represents and incorporates the effects of the system's geometry and the attenuation image determined from the active CT scan. \mathbf{A} is given by

$$A(E, s, \theta) = \iint a(E, x, y, s, \theta) \times \delta(x \cos \theta + y \sin \theta - s) dx dy. \quad (12)$$

The matrix \mathbf{A} can be calculated, but is too large to be inverted to solve for \mathbf{p} . Therefore, \mathbf{p} must be determined from \mathbf{g}_γ and \mathbf{A} using an iterative optimization technique.

3.1. Model and optimization codes

The iterative A&PCT reconstruction codes are divided into optimization and model codes [28,29]. The optimizer has a cost function and a minimizer algorithm. The former calculates a scalar by comparing the measured, \mathbf{g}_γ , to the calculated, $\hat{\mathbf{g}}_\gamma$; the latter searches for the next best solution, $\hat{\mathbf{p}}$. The optimizer determines when the solution is acceptable, the final $\hat{\mathbf{p}}$. The model code calculates

the system matrix \mathbf{A} and determines the calculated passive sinogram from the minimizer's current solution. It calculates the values in \mathbf{A} determined by the geometry and physics that relate the emission contribution from each voxel to the detector position, and includes attenuation from the ACT data. Our first model was developed in collaboration with UCSF [30].

In a waste drum gamma-rays produced by the decay of radioactive materials are best modeled by a Poisson probability distribution. Our version of the maximum likelihood for a Poisson distribution was called the Maximum Likelihood Expectation Maximization (MLEM) method [31]. Most of the results described in this paper were obtained using the UCSF-MLEM method [32]. However, it handles only one Poisson distribution signal, and in our case there are two Poisson distributions, gross and background counts [33]. We developed a more accurate algorithm that uses both the gross and background Poisson distributions in the assay [29].

4. Technology practice

4.1. Technology hardware

Four components constitute an A&PCT scanner. A radioactive source is used to acquire ACT attenuation data. Both the ACT and PCT measurements require an energy discriminating detector; we used a $\sim 90\%$ efficient [relative to a $7.6\text{ cm} \times 7.6\text{ cm}$ diam. NaI(Tl) detector at 1.3 MeV] HPGe detector. A computer-controlled stage translates and rotates a drum; and elevates either the drum, or the source and detector together, to enable data acquisition in a CT fashion. A computer carries out data acquisition, image processing, reconstruction and assay calculations.

Simulation studies examined the trade-off between data acquisition time, spatial resolution and signal-to-noise [34]. For example, to improve the spatial resolution by a factor of two would require that the measurement time be increased by a factor of eight. Our simulation studies showed that detector collimator apertures from $2.5\text{ cm} \times 2.5\text{ cm}$

to $7.5\text{ cm} \times 7.5\text{ cm}$ with an aspect ratio (aperture length divided by width) of 5:1–10:1 performed best. The smaller the aspect ratio the closer the HPGe detector is to a drum and the larger the solid angle it subtends. Since HPGe detectors with high counting efficiency are $\sim 8.2\text{ cm}$ outer diameter, we chose a $5.08\text{ cm} \times 5.08\text{ cm}$ aperture.

Two measurement modes constitute a typical A&PCT scan. First, collimated gamma-ray scanning (CGS), which is similar in data acquisition to segmented gamma scanning [1], quickly determines the matrix attenuation properties, general location of radioactivity and source activity versus height. In active CGS the transmission source is opened and data for pre-set EROI's are acquired. In passive CGS the source is shuttered and the entire spectrum is recorded. In effect, CGS defines the number of slices and ray sum integration times to be used in the second mode, the ACT and PCT scans described below.

4.2. Experimental systems

Here we describe two different A&PCT systems that were used to acquire several data sets to determine the performance of this technique. An R&D scanner was developed at LLNL for the assay of 208-l drums. This scanner was called IMPACT—*isotope measurements by passive and active computed tomography* [35]. It used a lead collimator for the HPGe detector that was 25.4 cm long [36] with a $5.08\text{ cm} \times 5.08\text{ cm}$ aperture. The radioactive source ($2.8\text{ mCi } ^{166\text{m}}\text{Ho} + 0.4\text{ mCi } ^{60}\text{Co}$) had a manual shutter and a 5.08 cm long lead collimator with a $2.54\text{ cm} \times 2.54\text{ cm}$ aperture. Between the source and detector was a three-axis stage that could translate a $<450\text{ kg}$ drum, elevate it $<1.25\text{ m}$, and rotate it step-wise or continuously through 360° .

For the ACT mode, drum translation was in 5.08 cm steps for each ray sum for a pre-set ray-sum integration time. A 208-l drum was translated 14 times over a distance of 71.12 cm and rotated about 8.5° over 180° (21 rotations). Each set of 14 ray sums made up a projection and 21 projections per ray sum completed a slice. After elevating 5.08 cm to a new slice plane, 21 new projections

were measured with 14 ray sums; and this measurement protocol continues for up to 18 slices, which are required to assay a full 208-l drum. Because of the increase acceptance angle in the PCT measurement we sometimes used only 7 ray-sums over 71.12 cm and 10 projections over 360° for each of the 18 slices [32,37]. The total time required for a complete A&PCT scan depends on drum fill height, number of ray sums and the ray-sum integration times used in both modes.

Seven regions in each summed PCT spectrum are analyzed for the closely spaced peak multiplets for the ratios: $^{238, 240} \text{Pu}/^{239} \text{Pu}$, $^{235} \text{U}/^{239} \text{Pu}$, and $^{241} \text{Am}/^{239} \text{Pu}$. In each region known energies and branching ratios are used to fix as many parameters as possible in the least squares fit. The goal is to generate a section of the spectrum mathematically from a set of peak shape parameters that closely approximate the measured net signal. The best fit gives a minimum reduced Chi squared difference between the calculated response and measured data. Details of our fitting process can be found in Refs. [32,38]. Analysis of the seven regions are combined with the assay data for $^{239} \text{Pu}$ (or $^{235} \text{U}$) to calculate the desired waste characterization parameters including mass ratios.

The second system was a technology transfer and collaborative effort between LLNL and BIR. This system was called waste inspection technology or WIT; and was integrated into a mobile trailer shown in Fig. 1 for field-deployed, production-mode [39] waste assays. WIT functions like IMPACT except in ACT the source and detector are pair-wise translated instead of the drum; while in PCT only the detector is translated. Trailer space limited the HPGe collimator to a 12.5 cm length, which required that ~2 mm thick septa be used to create four 2.5 cm × 2.5 cm effective apertures, each with an aspect ratio of 5:1. Because of the HPGe collimator's septa, experimental HPGe response functions were measured as a function of energy using a $^{152} \text{Eu}$ point source located at three distances (near and far from the detector and on the stage axis) from the HPGe detector vs. translational positions transverse to the HPGe axis. Several energy dependent HPGe response functions were incorporated into WIT's image reconstruction and assay code.

4.3. Performance criteria

The US DOE has defined the characterization criteria that will evaluate the ability of newly developed NDA technologies to meet repository site requirements for waste drums. They are stated in the National TRU Program's Quality Assurance Program Plan⁷ (QAPP) [41]; it states the data quality necessary to meet the Waste Isolation Pilot Plant's (WIPP) TRU waste quality assurance objectives (QAO). Parameters required for each technology are the measured accuracy of the total TRU alpha-Curie (α -Ci) content (percent recovery, %R) and precision (percent relative standard deviation, %RSD); and the technology's minimum detectable concentration (MDC) and total measurement uncertainty. Finally, an NDA assay system must demonstrate its capability over all types of wastes that it seeks to characterize.

The QAPP requires facilities using NDA systems to participate in a Performance Demonstration Program (PDP). This Program provides independent quality assurance of system performance [42,43]. The PDP consists of periodic blind tests (cycles) conducted using one or two different waste matrices coupled with simple and complex sources. The IMPACT system participated in PDP cycle 2 informally and passed PDP cycle 3 formally; the WIT system passed cycles 3 through 5 formally, all on the initial trial. WIT also participated in the Capability Evaluation Project (CEP) [44], which was a blind test study using wastes contaminated with TRU radioactivities. It was conducted at the INEEL⁸ using stored real wastes and surrogate drums, which are carefully constructed mock-waste matrices with known radioactive source amounts and locations. WIT also participated in a DOE-sponsored Rapid Commercialization Initiative (RCI), which utilized real and surrogate waste drums representative of INEEL wastes [45]. The scoring formalism of the PDP was applied to WIT in both the CEP and

⁷ The QAPP has been replaced by the Waste Acceptance Plan [40]. However since the work presented here fell under the QAPP we provide a summary of its requirements.

⁸ INEEL is Idaho National Engineering and Environmental Laboratory.

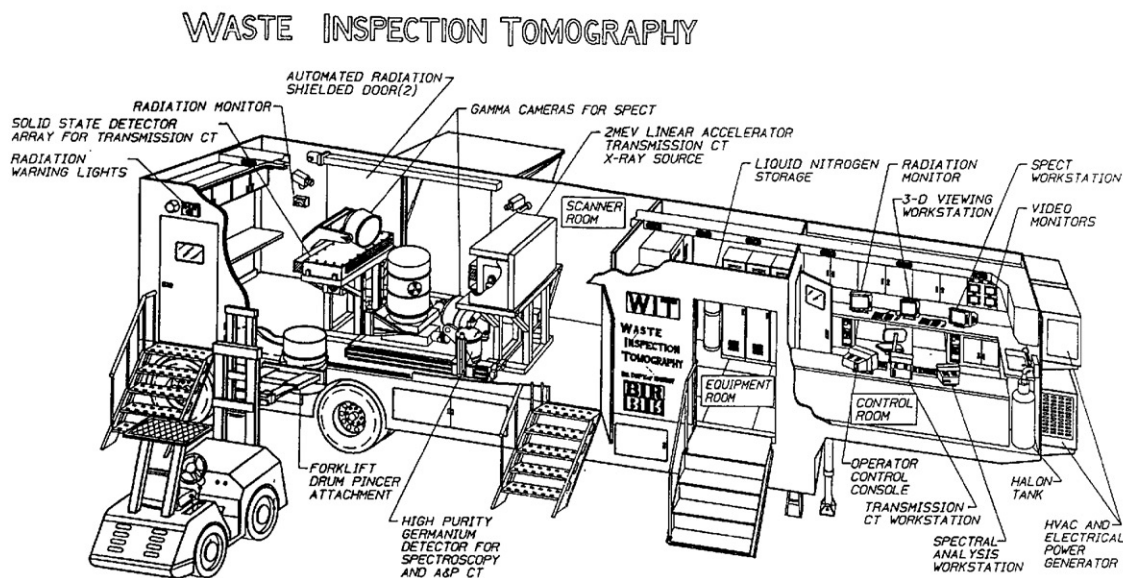


Fig. 1. BIRs mobile waste inspection trailer and a schematic layout of its equipment.

RCI studies with minor modifications, which allowed compliance and performance evaluations to be made.

5. Results

Both the IMPACT and WIT systems were used to measure real wastes at LLNL; and WIT was also tested at RFETS,⁹ INEEL and NTS.¹⁰ Many drums at LLNL contained multiple 4- and 20-l containers of solidified radioactive wastes. RFETS

wastes were all low-density combustibles. INEEL wastes included both lead-lined and normal drums containing matrices of graphite, glass, metals, sludge, and wet and dry combustibles. The NTS wastes were mostly combustibles. The amount of radioactivity assayed in waste drums for these sites ranged from 1 to 100 g of ²³⁹Pu. The results reported here used only known waste configurations and National Institute of Standards and Technology (NIST) standard emission sources.

5.1. IMPACT

Although the LLNL site formally participated in PDP Cycle 2, neither the IMPACT nor the WIT

⁹ RFETS is Rocky Flats Environmental and Technology Site.

¹⁰ NTS is Nevada Test Site.

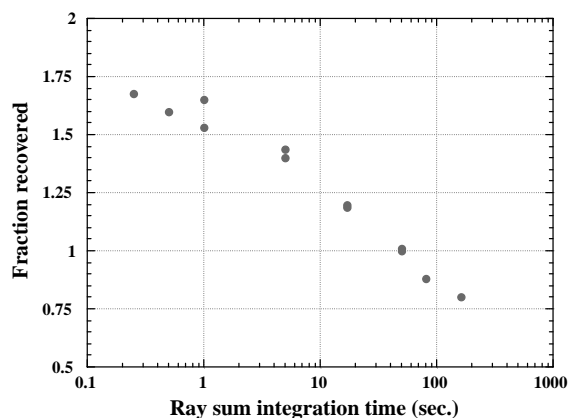


Fig. 2. IMPACT assay results using UCSF-MLEM for the PDP cycle 2 ethafoam drum with 0.93 g of WG Pu. Some integration times were repeated. Fraction recovered is our measured result relative to true.

system participated in this Cycle. However, we were able to use the Cycle 2 ethafoam¹¹ drum for our research. This drum was loaded with 0.93 g of WG Pu [46]. We used a 10 s ACT ray sum time to map its attenuation. Then, we ran many PCT scans ($14 \times 21 \times 17$ -slices) using the different ray sum times shown in Fig. 2. As integration time decreases assayed gram values increase. This occurred because the reconstruction code had a positivity constraint that ignored any “negative” net ray sum counts. This forced the reconstruction code to view spurious positive counts in a ray sum as valid data; and therefore, it must put intensity in corresponding voxels. In effect, UCSF-MLEM arbitrarily throws away the negative ray sum data that should have been used in the reconstruction algorithm to average the corresponding voxels to zero. Normally, we would expect that the ray sums from those voxels that have no source present would produce spurious positive and negative net counts that would average to zero. This positivity constraint led to the development of our constrained conjugate gradient (CCG) optimization code [29], which simultaneously solves for net and background contributions and reduced the observed positive assay bias [28] reported here. Drum

¹¹This drum matrix is no longer used in the PDP because it causes interference when neutron measurements are made.

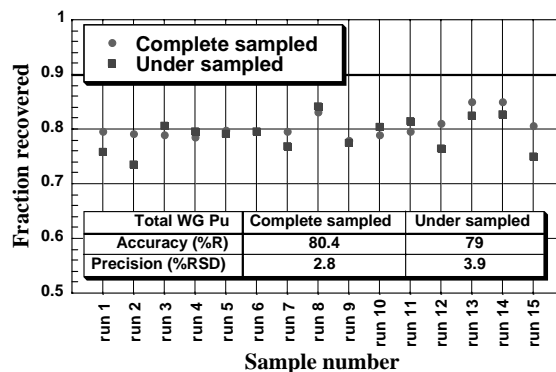


Fig. 3. Fifteen replicate measurement results from IMPACT using UCSF-MLEM for the combustible drum PDP003 containing 3.6 g WG Pu. Complete-(14 rays, 21 projections and 9 slices) and under-(7 rays, 10 projections and 9 slices) sampled data are shown.

activity coupled with the severity of matrix attenuation determines the optimum ray-sum integration time required to reduce this bias. For high activity drums a positive bias was not observed using UCSF-MLEM.

Fifteen replicate A&PCT scans were made of a combustible-matrix drum loaded with 3.6 g of WG Pu. These results are shown in Fig. 3. The ACT ray-sum time was 15 s. Results for a completely sampled PCT data set ($14 \times 21 \times 9$ -slices) with a ray sum time of 25 s gave a 80.4% recovery accuracy (%R) with a 2.8% relative standard deviation (%RSD), which satisfied the QAPP. Although one can use $14 \times 21 \times 18$ -slices to completely sample a drum in the PCT mode, fewer ray sums and projections can be used since the acceptance angle of the HPGe collimator aperture is larger in PCT than in ACT. Thus, to more efficiently sample a drum and do so in less time, we analyzed several data sets generated by computationally under-sampling their respective completely sampled data. For the 3.6 g drum, this resulted in an accuracy of 79% with a 3.9% RSD, which also satisfied the QAPP. Additional experiments verified that more efficient sampling gave similar results as complete sampling.

The PDP cycle 3 consisted of a combustible drum loaded with 71.36 g of WG Pu and a glass-matrix drum loaded with 98.3 g of WG Pu [47]. ACT scans ($14 \times 21 \times 17$ -slices) used a 6 s ray-sum

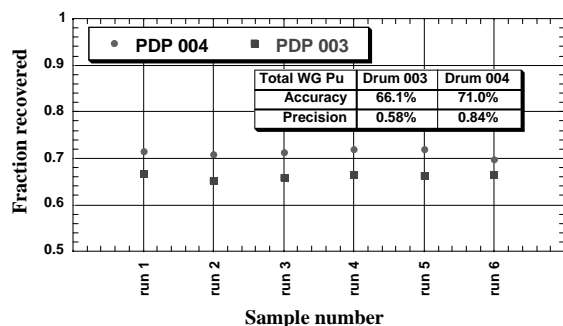


Fig. 4. IMPACT assay results using UCSF-MLEM for combustible (PDP003) and glass (PDP004) matrices containing 71.36 and 98.3 g of WG Pu, respectively.

time; PCT ($7 \times 9 \times 17$ -slices) a 20 s ray sum time. The results in Fig. 4 show that IMPACT using the UCSF-MLEM algorithm had a 30% low bias; i.e., a 66.1% accuracy with a 0.58% RSD on the combustible drum, and 71.0% accuracy with a 0.84% RSD on the glass drum. These results differ slightly from those reported in PDP Cycle 3 [47]; nevertheless in either case, the results were sufficiently accurate to pass the PDP requirements. A 3D surface-rendered image of the 414-keV radiation from the cylindrical ^{239}Pu sources in the glass drum (PDP004) is shown in Fig. 5. Two more PCT measurements at 10 and 5 s ray sum integration times were made on the glass matrix to test the system bias at shorter integration times. The percent recovery or accuracy results were 69.1 and 69.4, respectively. These values agree to better than 3% of the 20 s assay accuracy of 71.0%. Thus, for PCT signals with good counting statistics assay results are independent of ray-sum integration time as expected.

5.2. WIT

Field and test conditions in CEP, RCI and PDP cycles 4 and 5 made it preferable for WIT to assay as many drums as possible in a limited time. Thus, the CGS and A&PCT scans were done in ~ 22 h, so that both NDE and NDA were done for each drum in one day (≤ 24 h). Occasionally, a high-attenuating or low-activity drum was scanned over a weekend (~ 100 h). Data were acquired and

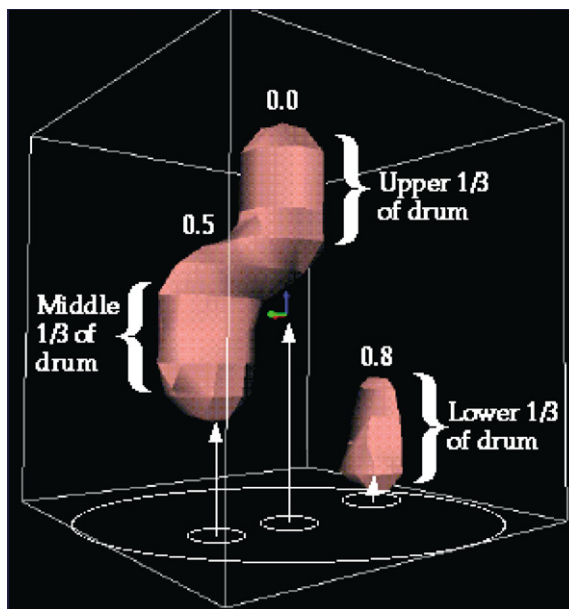


Fig. 5. A 3D surface rendered PCT image of the ^{239}Pu (414 keV) source distribution in the PDP cycle 3 glass-matrix drum (PDP004). The cylindrical standards (5 cm diameter \times 23 cm long) consisted of WG Pu: 65 g at 0 R (R is the drum radius), 30 g at 0.5 R, 3 g at 0.8 R, and 0.3 g at 0 R at a height from the bottom of the drum of 40.6, 17.8, 0, and 12.7 cm, respectively. The smallest standard was not recovered.

analyzed on BIRs trailer by technicians; LLNL reviewed all data acquired to provide the isotopics for each final report.

The RCI drum surrogates contained glass, combustible, and metals with 2.22, 0.933 and 0.747 g of ^{239}Pu , and 6.96, 1.01, and 0.804 mg of ^{241}Am , respectively. The real TRU wastes for RCI were in graphite, combustible, Raschig rings, and filter matrices with 24.4, ~ 0.02 , 10.1, and 76.3 g of ^{239}Pu , and 36, 0.03, 50, and 280 mg of ^{241}Am , respectively. The real waste-drum mass values are based on best estimates as acquired via the SWEPP¹² NDA system; and therefore, have an uncertainty with them. Thus, the precision required for scoring the RCI data were estimated from WITs participation in the PDP and CEP tests.

¹²SWEPP is the Stored Wastes Experimental Pilot Plant located at the INEEL.

Table 1
Summary of WIT performance in RCI test for total alpha activity using the UCSF-MLEM code

Test drum ID	Waste ID code no.	Precision WIT %RSD (σ/A_t) ^a	Precision QAO (%RSD)	Total α -Ci avg. %R (A_m/A_t) ^d	% Recovery acceptance criteria (95% confidence bounds)		²³⁹ Pu (%R)
					Lower (%R)	Upper (%R)	
1RF	300 (graphite)	7.1	<7.0	127	57.4	142.6	122.0
2RF	336 (moist combustibles)	—	<18.0	Below DL	—	—	Below DL
1SG	440 (glass)	3.89	<14.0	141.4 ^b	32.2	197.8	139.7 ^b
3RF	442 (Raschig ring)	2.95	<14.0	122	33.1	196.9	133.0
2SG	330 (dry combustibles)	4.15	<14.0	162.5 ^b	32.5	197.5	149.9 ^b
4RF	376 (filters/insulation)	1.54	<7.0	86	51.6	148.4	91.0
3SG	480 (metals)	4.15	<14.0	179.6 ^b	33.5	196.5	174.0 ^b
5RF ^c	001 (inorganic sludge)	2.73	<7.0	14.9 ^d	51.2	148.8	107.0

^a σ is the standard deviation, A_t is the true activity and A_m is the average measured activity.

^b These results have a high bias since the ray-sum integration times were too short (see Section 5.1).

^c Data for drum 5RF was not fully evaluated by INEEL at the time of this test.

^d The reason for this low result is unknown. It may be due to a high loading of ²⁴¹Am, which was not measured during these tests.

Table 2
Summary of WIT performance in the CEP test for total alpha activity using the UCSF-MLEM code

Test drum ID	Waste ID code no.	Precision WIT %RSD (σ/A_t) ^a	Precision QAO (%RSD)	Total α -Ci avg. %R (A_m/A_t) ^a	Total α avg. % recovery acceptance criteria (95% confidence bounds)	²³⁹ Pu (avg. %R)	²⁴¹ Am (avg. %R)	²³⁵ U (avg. %R)	²³⁸ U (avg. %R)
Surrogates					Lower (%R)	Upper (%R)			
SG6	409 (MSE Salts)	1.1	<7.0	70.7	50.9	149.1	103.5	15.4	—
SG9	442 (Raschig ring)	4.2	<14.0	154.9	33.5	196.5	146.0	284.4	—
RFETS									
RF11 ^b	003 (organic sludge)	5.0	<14.0	161.4	35.0	195.0	144.9	141.9	0.0
RF11 ^c	003 (organic sludge)	5.9	<14.0	191.0	35.9	194.1	183.8	242.9	0.0
RF20	480 (metals)	0.8	<14.0	96.8	30.7	199.3	121.2	28.9	0.0

^a σ is the standard deviation, A_t is the true activity and A_m is the average measured activity.

^b Active neutron-based measured mass evaluation.

^c Radiochemistry evaluation.

The RCI results are presented in Table 1. The average RCI total alpha-Curie %R and %RSD are 119 and 3.8, respectively. Analysis of the ^{239}Pu %R for drum mass loadings greater than 3 g yields a mean %R of 115; while for the three drums (excluding 2RF) with ^{239}Pu masses less than 3 g, analysis yields a mean %R of 154. Thus, these data reflect the same trend as shown in Fig. 2, i.e., the lower the loading the higher the bias for short, fixed integration times.

The CEP consisted of surrogate drums constructed with metals, molten salts, Raschig rings, and sludge loaded with 3.97, 46.0, 0.961, and 1.53 g¹³ of ^{239}Pu , respectively; and the CEP tests required eight replicates of each drum [3]. The CEP results are shown in Table 2 and suggest that WITs mean Total α -Ci %R is about 25% high. The excellent recovery of 104% for the 46 g of ^{239}Pu in the molten salts drum, SG6, are offset by the very-high mean recovery of 164% for the 1.5 g in the sludge matrix. This high biased value is consistent with the early IMPACT results and the WIT RCI test results when insufficient ray sum integration times are used.

The PDP combustible and empty waste drums from cycle 4 were loaded with 6.66 and 98.3 g of WG Pu, or 6.16 and 92.27 g of ^{239}Pu , respectively. The test results are summarized in the PDP report for cycle 4 [48]. The total alpha-Curie %R and %RSD are 99.1 and 1.54, and 109.8 and 2.95 for the empty and combustible drums, respectively, which yield means of 104.5 and 2.25, respectively.

The PDP cycle-5A consisted of waste drums containing a combustible and a sludge matrix and were loaded with 0.314 and 0.546 total alpha-Curie, respectively. The test results are summarized elsewhere [49]. The total alpha-Curie %R and %RSD are 96.1 and 2.1, and 101 and 4.3 for the combustible and sludge drums, respectively, which yield means of 98.5 and 3.2, respectively. These results are the only ones obtained using the new constrained conjugate gradient algorithm [29,33].

Table 3

Radionuclides identified in waste by WIT

U & TRU	Other actinides ^a	Other radionuclides—source
^{235}U	^{208}Tl	^{22}Na —F(α ,p)
^{238}U	^{219}Rn	^{40}K —bckgd.
$^{237}\text{Np}^a$	^{223}Ra	^{60}Co —fp ^b
$^{238}\text{Pu}^c$	^{227}Th	^{137}Cs —fp
^{239}Pu	^{243}Cm	^{211}Pb —bckgd.
^{240}Pu	^{249}Cf	^{214}Bi —bckgd.
^{241}Pu		
^{241}Am		

^a Primarily identified in LLNL waste drums at NTS; some were identified in drums at LLNL, RFETS and INEEL.

^b fp means a fission product derived isotope.

^c ^{238}Pu can be seen in wastes enriched in this isotope, but most waste drums contain WG Pu; thus ^{238}Pu 's percentage abundance is too small for its gamma-rays to be detected.

5.3. Summary of results

Those radioactive isotopes detected during the WIT tests at all sites [50] are presented in Table 3. A summary of IMPACT and WIT scanner performances results in terms of ^{239}Pu mass for the %R and %RSD are given in Table 4. Here we only report the ^{239}Pu mass results for surrogate drums since the ^{239}Pu mass within them is precisely known and NIST traceable. Some CEP and RCI results for real wastes are excluded from Table 4 since their ^{239}Pu gram mass remains uncertain. The average %R and %RSD for IMPACT is 69 and 0.7, respectively. This negative 30% bias for IMPACT using the UCSF-MLEM code was reduced to a negative 10% when the APCT-CCG code [32] was used on the same data.

The overall average %R and %RSD for WIT is 124 and 2.6, respectively. Five of the nine WIT scanner results are within 10% of the true value. The two results near 148% and the one result at 174% are most likely due to an insufficient counting time for the ^{239}Pu mass content, and yield a large positive bias as discussed above when the UCSF-MLEM code is used.

6. Conclusion

We have demonstrated that active and passive computed tomography can localize, quantify and

¹³ This value is the average of two different assay measurements—the radiochemistry and SWEPP active neutron-based NDA values of 1.35 and 1.71 g of ^{239}Pu , respectively.

Table 4
IMPACT and WIT blind test results for surrogate drums using UCSF-MLEM^a

Test system ^b Drum	No. of Rep. ^c (²³⁹ Pu g) ^d	Sample ID (matrix)	Measurement	
			%R for ²³⁹ Pu mass	%RSD ²³⁹ Pu mass
IMPACT	6	Drum 003	66.1	0.58
PDP-3	(66.87)	(Combustibles)		
IMPACT	6	Drum 004	71.0	0.84
PDP-3	(92.11)	(Glass)		
WIT	1	1-SG	140	2.8 ^e
RCI	(2.22)	(Glass)		
WIT	1	2-SG	150	2.7 ^f
RCI	(0.933)	(Comb.)		
WIT	1	3-SG	174	2.7 ^f
RCI	(0.747)	(Metals)		
WIT	6	Drum 003	110	2.9
PDP-4	(6.16)	(Combustibles)		
WIT	6	Drum 001	98.7	2.1
PDP-4	(92.27)	(Zero)		
WIT	6	Drum 003	96.1 ^g	2.1
PDP-5A	(—)	(Combustibles)		
WIT	6	Drum 005	101 ^g	4.3
PDP-5A	(—)	(Sludge)		
WIT	8	SG-6	104	1.5
CEP	(46.0)	(MSE Salt)		
WIT	8	SG-9	146	2.7
CEP	(0.961)	(Raschig)		

^aThe results for the WIT PDP-5A drums were obtained using the CCG algorithm.

^bThe RCI and CEP tests were both conducted and scored by INEEL. The PDP tests were scored by DOE-CAO [46–48].

^cNumber of replicate scans.

^dActual ²³⁹Pu content in grams.

^eWITs %RSD determined from IMPACT's 15 replicate QAO test using 3.6 g of WG Pu.

^fWITs %RSD was determined from the CEP test sample SG-9 with 0.961 g of ²³⁹Pu.

^gThese %R values are total alpha-Curie values, not just ²³⁹Pu mass values.

identify TRU isotopes independent of the waste matrix. This technology provides images for both the radioactive materials and the gamma-ray attenuation of the waste versus energy in a voxel size of 131 cm³ (i.e., 5.08 cm × 5.08 cm × 5.08 cm) of a 208-l drum. The A&PCT technology removes nearly all of the biases arising from nonuniform radioactivity and the surrounding waste matrix distributions. Coupling a fast drum CGS prescan with A&PCT provides drum measurement times that are scalable to activity amount, waste-matrix density and drum fill-height. This approach ensures that a predesired accuracy and precision are obtained in the shortest possible measurement time.

We further demonstrated the successful transfer of the A&PCT technology from R&D to a commercially based, mobile system. Both the laboratory-based A&PCT system (IMPACT) and the mobile system (WIT) participated in and passed all performance tests entered to date. Calibration of the A&PCT technology consists simply of a single measurement of a NIST traceable radioactive source at a known detector distance. Its calibration does not require the use of any surrogate waste matrix drums or assorted reference sources; and this technology does not require that waste drums be segregated according to their waste type before they are assayed. Thus, all waste drums can be nondestructively assayed

one after the other without regard to their activity level, gamma-ray emitting isotopes or waste matrix content.

Two future developments that might further improve waste drum characterization would be “smart” scanning and data fusion. An example of “smart” scanning would be to take only one ACT ray sum scan for a near homogeneous waste matrix (e.g., sludge) since it has nearly a constant attenuation per unit length, and is all that is needed to correct the PCT emission data. Data fusion might further improve waste characterization if results from an NDE X-ray transmission CT scan, which provides higher-spatial resolution of drum contents, were integrated with assay results from both tomographic gamma-ray and neutron imaging systems.

Acknowledgements

We thank Steve Azevedo, Gene Ford, Linwood Hester, Erik Johansson, Eric Keto and Sailes Sengupta at LLNL for their many contributions during various development stages of this A&PCT technology. We also thank David Enwistle and David Nisius at BIR for their support of our R&D effort. The LLNL research and development work was supported by the DOE Environmental Management program. The transfer of the A&PCT technology to BIR and their part of this work was funded by Programmatic Research and Development Agreements (PRDA) from National Energy Technology Laboratory, Morgantown, WV. The LLNL work was performed under the auspices of the US Department of Energy by The University of California Lawrence Livermore National Laboratory under contract No. W-7405-ENG-48.

References

- [1] R. Martin, D.F. Jones, J.L. Parker, Gamma-ray measurements with the segmented gamma scanner, LA-7059-M, Los Alamos Scientific Laboratory, 1977.
- [2] J.T. Caldwell, R.D. Hastings, G.C. Herrera, W.E. Kounz, E.R. Shrunk, The Los Alamos second generation system for passive and active neutron assays of drum size containers, LA-10774-MS, Los Alamos Scientific Laboratory, 1986.
- [3] M.E. McIlwain, G.K. Becker, Nondestructive waste assay capability evaluation program, Proceedings of the Sixth Nondestructive Assay and Nondestructive Examination Waste Characterization Conference, Salt Lake City, Utah, November 17–19, 1998, CONF-981105, pp. 171–190.
- [4] R.T. Bernardi, H.E. Martz, Jr., Nuclear waste drum characterization with 2 MeV X-ray and gamma-ray tomography, Proceedings of the SPIE's 1995 International Symposium on Optical Science, Engineering, and Instrumentation, Vol. 2519, San Diego, CA, July 13–14, 1995.
- [5] H.E. Martz, D.J. Decman, G.P. Roberson, D.C. Camp, R.T. Bernardi, Radioactive waste realities as revealed by X- and gamma-ray measurements, American Chemical Society 1995, Extended Abstracts for the Special Symposium on Emerging Technologies in Hazardous Waste Management VII, Atlanta, GA, September 17–20, 1995, pp. 889–894.
- [6] G.P. Roberson, H.E. Martz, D.J. Decman, J.A. Jackson, R.T. Bernardi, D.C. Camp, Nondestructive assay using active and passive computed tomography, Presented at the INMM 39th Annual Meeting, Naples, FL, July 26–30, 1998.
- [7] H.E. Martz, G.P. Roberson, K. Hollerbach, C.M. Morgan, E. Ashby, R.T. Bernardi, Computed tomography of human joints and radioactive waste drums, in: R.E. Green (Ed.), Proceedings of Nondestructive Characterization of Materials™ IX; Sydney Australia, June 28–July 2, 1999; AIP Conference Proceedings 497; Melville, NY, pp. 607–615.
- [8] G.P. Roberson, H.E. Martz, D. Nisius, Active and passive computed tomography for nondestructive assay, Proceedings for the American Nuclear Society 1999, Winter Meeting and Embedded Topical Meetings, Long Beach, CA, Vol. 81, November 14–18, 1999, pp. 229–231.
- [9] D. Nisius, R.T. Bernardi, Performance tests of the WIT 6-detector gamma NDA system, Proceedings of the Seventh NDA Waste Characterization Conference, Salt Lake City, UT, May 23–25, 2000, INEL CONF-2000-0002, pp. 627–638.
- [10] D.C. Hensley, An overview of the ORNL-NFS intercomparison, Proceedings of the Fifth Nondestructive Assay and Nondestructive Examination Waste Characterization Conference, Salt Lake City, Utah, January 14–16, 1997, INEL CONF-970126, p. 93.
- [11] R.A. Hogle, P. Miller, R.L. Bramblett, APNEA list mode data acquisition and real-time event processing, Proceedings of the Fifth Nondestructive Assay and Nondestructive Examination Waste Characterization Conference, Salt Lake City, Utah, January 14–16, 1997, INEL CONF-970126, p. 183.
- [12] C.L. Hollas, G. Arnone, G. Brunson, K. Coop, Matrix effects corrections in DDT assay of ^{239}Pu with the CTEN instrument, Proceedings of the Fifth Nondestructive Assay and Nondestructive Examination Waste Characterization Conference, Salt Lake City, Utah, January 14–16, 1997, INEL CONF-970126, p. 175.

- [13] R.J. Estep, T.H. Prettyman, G.A. Sheppard, Nucl. Sci. Eng. NS-118 (1994) 145.
- [14] T.H. Prettyman, S.E. Betts, D.P. Taggart, R.J. Estep, N.J. Nicholas, M.C. Lucas, R.A. Harlan, Field experience with a mobile tomographic nondestructive assay system, LA-UR-95-3501, Los Alamos National Laboratory, Los Alamos, NM, October 1995.
- [15] J. Gregor, D.C. Hensley, Gamma-ray imaging of the quincy sources, Proceedings of the Fifth Nondestructive Assay and Nondestructive Examination Waste Characterization Conference, Salt Lake City, UT, January 1997, INEL CONF-970126, p. 361.
- [16] G.K. Becker, J.C. Determan, Application of expert system technology to nondestructive waste assay—initial prototype model, Proceedings of the Fifth Nondestructive Assay and Nondestructive Examination Waste Characterization Conference, Salt Lake City, Utah, January 14–16, 1997, INEL CONF-970126, p. 455.
- [17] M.M. Pickrell, D.J. Mercer, T.J. Sharpe, A technique for combining neutron and gamma-ray data into a single assay value, Presented at the INMM 39th Annual Meeting, Naples, FL, July 26–30, 1998 and LA-UR-98-3203, Los Alamos National Laboratory, Los Alamos, NM.
- [18] H. Gotoh, Japan Atomic Energy Research Institute, Tokai-Mura, Naka-Gun, Ibaraki-ken 319-11 Japan, private communication, 1991.
- [19] P. Reimers, Quality Assurance of Radioactive Waste Packages by Computerized Tomography, Task 3, Characterization of Radioactive Waste Forms; A Series of Final Reports (1985–1989)—No. 37, Nuclear Science and Technology, EUR 13879 EN, Commission of the European Communities, Luxembourg, 1992.
- [20] S. Kawasaki, M. Kondo, S. Izumi, M. Kikuchi, Appl. Radiat. Isot. 41 (1990) 983.
- [21] P. Eifler, E. Metz, R. Odoj, Determination of the nuclide inventory of radioactive waste barrels by using a tomographic method, Proceedings of the International Symposium on Computerized Tomography for Industrial Applications, 8–10 June 1994, Berlin, DGZfp.
- [22] F. Lévai, Z.S. Nagy, T.Q. Dung, Low resolution combined emission-transmission imaging techniques for matrix characterization and assay of waste, Proceedings of the 17th ESARDA Symposium, Aachen, May 1995, pp. 319–323.
- [23] C. Robert-Coutant, V. Moulin, R. Sauze, Ph. Rizo, Estimation of the matrix attenuation in heterogeneous radioactive waste drums using dual-energy computed tomography, Presented at 1998 Symposium on Radiation Measurements and Applications, May 11–14, 1998, Ann Arbor, MI, pp. 949–956.
- [24] Proceedings of the Fourth Nondestructive Assay and Nondestructive Examination Waste Characterization Conference, Salt Lake City, Utah, October 24–26, 1995, INEL CONF-951091; Proceedings of the Fifth Nondestructive Assay and Nondestructive Examination Waste Characterization Conference, Salt Lake City, Utah, January 14–16, 1997, INEL CONF-970126; Proceedings of the Sixth Nondestructive Assay Waste Characterization Conference, Salt Lake, Utah, November 17–19, 1998, INEL-CONF-981105; Proceedings of the Seventh Nondestructive Assay Waste Characterization Conference, Salt Lake, Utah, May 23–25, 2000; INEL CONF-2000-0002.
- [25] T.F. Budinger, G.T. Gullberg, R.H. Huesman, Emission computed tomography, in: G.T. Herman (Ed.), *Image Reconstruction from Projections Implementation and Applications*, Springer, New York, 1979, p. 147.
- [26] A.C. Kak, M. Slaney, *Principles of Computerized Tomographic Imaging*, IEEE Press, New York, 1988.
- [27] G.T. Herman, *Image Reconstruction from Projections*, Academic Press, New York, 1980.
- [28] G.P. Roberson, H.E. Martz, D.J. Decman, J.A. Jackson, D. Clark, R.T. Bernardi, D.C. Camp, Active and passive computed tomography for nondestructive assay, Sixth Nondestructive Assay and Nondestructive Examination Waste Characterization Conference, Salt Lake City, Utah, November 17–19, 1998, p. 359.
- [29] J.A. Jackson, D. Goodman, G.P. Roberson, H.E. Martz, An active and passive computed tomography algorithm with a constrained conjugate gradient solution, Proceedings of the Sixth Nondestructive Assay Waste Characterization Conference, Salt Lake City, UT, November 127–19, 1998, pp. 325–358.
- [30] J.K. Brown, K. Kalki, J.A. Heanue, B.H. Hasegawa, Conference Record 1995 IEEE Nuclear Science Symposium and Medical Imaging Conference 2 (1995) 1272.
- [31] L.A. Shepp, Y. Vardi, IEEE Trans. Med. Imaging, MI-1(2) (1982).
- [32] H.E. Martz, G.P. Roberson, D.C. Camp, D.J. Decman, J.A. Jackson, G.K. Becker, Active and passive computed tomography, Mixed Waste Focus Area Final Report, Lawrence Livermore National Laboratory, Livermore, CA, UCRL-ID-131695, November 1998.
- [33] D.M. Goodman, Maximum likelihood estimation with Poisson (Counting) statistics for waste drum inspection, UCRL-ID-127361, Lawrence Livermore National Laboratory, Livermore, CA, May 1997.
- [34] E. Keto, S. Azevedo, P. Roberson, D. Decman, H. Martz, E. Johansson, Spatial resolution versus signal to noise in quantitative tomography, Proceedings of the Fourth Nondestructive Assay & Nondestructive Examination Waste Characterization Conference, Salt Lake, Utah, October 24–26, 1995, pp. 405–420.
- [35] G.P. Roberson, H.E. Martz, D.J. Decman, D.C. Camp, S.G. Azevedo, E.R. Keto, Characterization of waste drums using nonintrusive active and passive computed tomography, Proceedings of the Fourth Nondestructive Assay and Nondestructive Examination Waste Characterization Conference, Idaho State University, Pocatello, Idaho, February 14–16, 1994, pp. 261–294.
- [36] D.J. Decman, H.E. Martz, G.P. Roberson, E. Johansson, *NDA via gamma-ray active and passive computed tomography*, Mixed Waste Focus Area Final Report, Lawrence Livermore National Laboratory, Livermore, CA, UCRL-ID-125303, November 1996.

- [37] G.P. Roberson, H.E. Martz, D.C. Camp, D.J. Decman, E.M. Johansson, Preliminary A&PCT Multiple Detector Design, Upgrade of a Single HPGe detector A&PCT System to Multiple Detectors, Lawrence Livermore National Laboratory, Livermore, CA, UCRL-ID-128052, June 1997.
- [38] D. Clark, D. Decman, Transuranic isotopic analysis using gamma rays, Presented at the Sixth Nondestructive Assay Waste Characterization Conference, Salt Lake City, Utah, November 17–19, 1998, pp. 243–258.
- [39] R.T. Bernardi, Field test results for radioactive waste drum characterization with waste inspection tomography (WIT), Proceedings of the Fifth Nondestructive Assay and Nondestructive Examination Waste Characterization Conference, Salt Lake City, Utah, January 14–16, 1997, INEL CONF-970126, p. 107.
- [40] Waste Acceptance Plan, EPA, DOE/WIPP-069, November 8, 1999, Rev 7.
- [41] Transuranic Waste Characterization Quality Assurance Program Plan, US Department of Energy, Carlsbad Area Office, National TRU Program Office, CAO-94-1010, Interim Change, November 15, 1996.
- [42] Performance Demonstration Program Plan for Non-Destructive Assay for the TRU Waste Characterization Program, US Department of Energy, Carlsbad Area Office, National TRU Program Office, CAO-94-1045, Revision 1, May 1997.
- [43] C.J. Marcinkiewicz, M.J. Connolly, G.K. Becker, Performance in the WIPP nondestructive assay performance demonstration program, Proceedings of the Fifth Nondestructive Assay and Nondestructive Examination Waste Characterization Conference, Salt Lake City, Utah, January 14–16, 1997, INEL CONF-970126, p. 175.
- [44] M.E. McIlwain, G.K. Becker, M.J. Connolly, Nondestructive waste assay capability evaluation program, Sixth Nondestructive Assay and Nondestructive Examination Waste Characterization Conference, Salt Lake City, Utah, November 17–19, 1998, p. 171.
- [45] R.T. Bernardi et al. Rapid Commercialization Initiative Final Report for The Waste Inspection Tomography, 96-RCI-09, DOE FETC, August 31, 1998.
- [46] Performance Demonstration Program Plan for Non-Destructive Assay for the TRU Waste Characterization Program, Scoring Report, November 1996 Distribution prepared by Lockheed Martin Idaho Technologies Company, Idaho Falls, ID, for US Department of Energy, Carlsbad Area Office, National TRU Program Office, January 1997.
- [47] Performance Demonstration Program Plan for Non-Destructive Assay for the TRU Waste Characterization Program, Scoring Report, May 1997 Distribution prepared by Lockheed Martin Idaho Technologies Company, Idaho Falls, ID, for US Department of Energy, Carlsbad Area Office, National TRU Program Office, July 1997.
- [48] Performance Demonstration Program Plan for Non-Destructive Assay for the TRU Waste Characterization Program, Scoring Report, September 1997 Distribution prepared by Lockheed Martin Idaho Technologies Company, Idaho Falls, ID, for US Department of Energy, Carlsbad Area Office, National TRU Program Office, November 1997.
- [49] C.J. Marcinkiewicz, Summary of System Performance in the WIPP Nondestructive Assay Performance Demonstration Program, Proceedings of the Seventh Nondestructive Assay and Nondestructive Examination Waste Characterization Conference, Salt Lake City, Utah, May 23–25, 2000, INEL /EXT-2000-0002, pp. 39–84.
- [50] Waste Inspection Tomography (WIT), Innovative Technology Summary Report, prepared for US Department of Energy, Office of Environmental Management DOE/EM-0579, and Office of Science and Technology OST/TMS ID 259, April 2001; see also <http://ost.em.doe.gov>, under publications.